UNIVERSALITY AND SCALING IN THE BEHAVIOR OF COUPLED FEIGENBAUM SYSTEMS

S. P. Kuznetsov

UDC 517.9

The behavior of two symmetrically coupled identical systems, each of which is separately capable of demonstrating transition to chaos through period doubling bifurcation, is investigated. Scaling relations are established, being the generalization of the Feigenbaum scaling laws to coupled systems. The universal configuration of different regime zones is found in the space of three parameters: the Feigenbaum control parameter and the coefficients of inertial and dissipative types of coupling.

The study of stochastic oscillations in dynamic systems has recently led to the formation of several universal models, describing the behavior of various systems near the threshold of generation of chaos [1-3]. One of these models, henceforth named the Feigenbaum system, is a generalized nonlinear dissipative system, undergoing transition to chaos during the variation of some control parameter λ through a hierarchy of period doubling bifurcations. As shown by Feigenbaum [1, 2], this transition obeys a number of universal scaling laws. In particular, the sequence of bifurcation points is determined by the equation

$$\lambda_m = \lambda_c - K\delta^{-m}, \tag{1}$$

where $\delta = 4.6692$ is a universal constant, and λ_c and K are constants depending on the specific system. This type of behavior is observed in numerical computations and in experiments on many specific systems in radiophysics, hydrodynamics, as well as chemical and biological models [4-7]. A natural path of constructing a theory consists in developing more complicated objects on the basis of the Feigenbaum system, such as systems with external action, coupled systems, a distributed medium [8-14], and in the study of order—chaos transition laws in them.

We turn to the problem of behavior of two identical symmetrically coupled elements, each of which is a Feigenbaum system. Specific examples can be coupled nonlinear oscillators under periodic external action, coupled cells undergoing self-catalytic chemical reactions, communicating biological populations, etc.

The simplest Feigenbaum systems is the recurrent equation [1]:

$$x_{n+1} = \lambda - x_n^2, \tag{2}$$

Saratov State University. Translated from Izvestiya Vysshikh Uchebnykh Zavedenii, Radiofizika, Vol. 28, No. 8, pp. 991-1007, August, 1985. Original article submitted May 14, 1984; revision submitted October 22, 1984.

0033-8443/85/2808-0681$09.50

where x_n characterizes the state of the system at the discrete moment of time n. The behavior of the two coupled systems (2) for several special methods of introducing coupling was investigated numerically in [9-11]. It was shown that the transition paths of coupled systems to chaos are richer than for individual elements: transitions through destruction of quasiperiodic motions and intermittence were observed besides period doubling. The studies [9-11], however, have left open principal questions concerning the clarification of the properties of coupled systems following from the Feigenbaum laws for the constituent elements, as well as explaining the extent of dependence of behavior of coupled systems on the specific method of introducing coupling.

The purpose of the present study is to address these problems. The study is based on the renormalized group (RG) approach, being a development of the analysis method earlier suggested for one-dimensional chains consisting of Feigenbaum systems [12, 13].

1. BASIC EQUATIONS

1.1. Qualitative Discussion of Methods of Introducing Coupling. A traditional example of a Feigenbaum system, described by Eq. (2), is biological population [2, 7]. In this case x_n characterizes the magnitude of the population (more exactly, its deviation from an extremum level) before the n-th cycle of multiplication and decomposition, and the parameter λ can be determined independently.

We use this example to illustrate the methods of introducing coupling between Feigenbaum systems. Consider initially two uncoupled populations of the same shape, whose magnitude is given by the variables x_n and y_n, evolving according to the equations

$$x_{n+1}=\lambda-x_n^2, \quad y_{n+1}=\lambda-y_n^2. \tag{3}$$

This situation is shown schematically in Fig. 1a. Each rectangle represents a cycle of multiplication and decomposition, corresponding to the nonlinear transformation of the population value, while the vertical lines represent the period of existence of population without change of magnitude.

Coupling between populations can be introduced by two substantially different methods. The first consists of the fact that at intermediate times between multiplication and decomposition periods there can be "gliding" in both sides of the coupling channel, as illustrated in Fig. 1b. This coupling is, obviously, capable of equating the instantaneous populations of both populations. If the population magnitude before the following cycle of multiplication and decomposition is given by the quantities x_n and y_n, then following this cycle they are given by the quantities $\lambda - x_n^2$ and $\lambda - y_n^2$. Assuming that then some fraction ε "slides" from its population to the population along the coupling channel, we find the variable values before the following cycle:

$$x_{n+1} = \lambda - x_n^2 + \varepsilon (x_n^2 - y_n^2), \quad y_{n+1} = \lambda - y_n^2 + \varepsilon (y_n^2 - x_n^2). \tag{4}$$

A coupling of this type can be called dissipative. Indeed, consider the transformation of phase space $\Delta x_n \Delta y_n$ after a unit time:

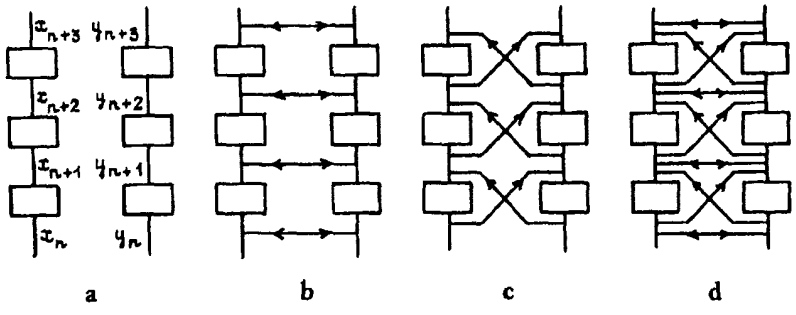

Fig. 1

$$\Delta x_{n+1}\Delta y_{n+1} = J\Delta x_n \Delta y_n,$$

where J is the Jacobian, namely,

$$J = \begin{vmatrix} \partial x_{n+1}/\partial x_n & \partial x_{n+1}/\partial y_n \\ \partial y_{n+1}/\partial x_n & \partial y_{n+1}/\partial y_n \end{vmatrix} = \begin{vmatrix} -2x_n(1-\varepsilon) & -2\varepsilon y_n \\ -2\varepsilon x_n & -2y_n(1-\varepsilon) \end{vmatrix} = 4x_n y_n(1-2\varepsilon).$$

In the absence of coupling $J_0 = 4x_n y_n$, while in the presence of coupling $J = (1 - 2\varepsilon)J_0$. Thus, when the condition $0 < \varepsilon < 1$, which is natural within the biological interpretation, is imposed on ε the phase volume undergoes further compression in comparison with the same quantity in the absence of coupling.

The second method of introducing coupling consists of obtaining the possibility of "gliding" from one population to another within a cycle of multiplication and decomposition, as shown in Fig. 1c. Denoting by μ the fraction starting to travel along the coupling channel, one obtains the following equations: $x_{n+1}=\lambda-(x_n-\mu x_n)^2+\mu y_n$, $y_{n+1}=\lambda-(y_n-\mu y_n)^2+\mu x_n$. Replacing $x \to \frac{x+\mu/2}{(1-\mu)^2}$, $y \to \frac{y+\mu/2}{(1-\mu)^2}$, $\lambda \to \frac{\lambda+\mu/2-\mu^2/4}{(1-\mu)^2}$, they lead to the form

$$x_{n+1}=\lambda-x_n^2+\mu(y_n-x_n), \quad y_{n+1}=\lambda-y_n^2+\mu(x_n-y_n). \tag{5}$$

The principal difference between the methods described of introducing coupling consists of the following. At some moment $\bar{n}$ let both variables occur near the extremum point of the mapping (2): $|x_{\bar{n}}| \ll 1$, $|y_{\bar{n}}| \ll 1$. Due to dissipative coupling the information on the different subsystem states will be lost at the moment $\bar{n}$ (the difference $y_{\bar{n}+1} - x_{\bar{n}+1}$ is proportional to the square of a small quantity). For the system (5), on the contrary, the information is not lost: the previous history of the system affects the subsequent behavior in bypassing the quadratic extremum through the coupling channel. This justifies calling the second type of coupling inertial. The definitions given here are preliminary, and will be refined in Section 2.

Let there now exist coupling channels of both types (Fig. 1d). If the coupling is weak, corrections to the right hand sides of Eqs. (3) must appear additively, so that we obtain directly

$$\begin{aligned} x_{n+1} &= \lambda - x_n^2 + \varepsilon(x_n^2 - y_n^2) - \mu(x_n - y_n), \\ y_{n+1} &= \lambda - y_n^2 + \varepsilon(y_n^2 - x_n^2) - \mu(y_n - x_n). \end{aligned} \tag{6}$$

It seems that other methods of introducing coupling need not be considered: for a suitable parameter choice Eqs. (6) guarantee adequate description of Feigenbaum systems, weakly coupled in an arbitrary manner (see below).

For what follows it is useful to introduce the variables $\xi_n = (x_n + y_n)/2$, $\eta_n = (x_n - y_n)/2$, characterizing the symmetric and antisymmetric parts of the solution. In the new variables Eqs. (6) acquire the form

$$\xi_{n+1}=\lambda-\xi_n^2-\eta_n^2, \quad \eta_{n+1}=-2B(\xi_n+\alpha)\eta_n, \tag{7}$$

where $B = 1 - 2\varepsilon$, $\alpha = \mu/(4\varepsilon - 2)$.

1.2. Scaling Laws. We turn now again to the system of uncoupled elements (3). The following scaling law follows from Feigenbaum's results [1, 2]:

a) Let it be known that for the parameter value $\lambda_c + \Lambda$ the system transforms from state (x, y) to state (X, Y) after 2^m units of time.

b) For the parameter value $\lambda_c + \Lambda/\delta$ it then transforms from state $(x/\alpha, y/\alpha)$ to state $(X/\alpha, Y/\alpha)$ after 2^{m+1} units of time, with $\delta = 4.6692$, $\alpha = -2.5029$.

In different words, if there exists any solution of system (3), then one can search a scaling regime with a time scale multiplied by two times. For this one must recalculate the

initial state (x, y) and the value of the parameter λ according to the rules given.

A similar scaling law must also exist for coupled systems, while with the exclusion of coupling it necessarily transforms to the statement given above. Therefore the rule of computing x, y, and λ must be retained, at least in the case of weak coupling. Consequently, the problem consists of identifying the rule of computing the function characterizing the coupling.

Consider initially system (5) (Fig. 1c). In transforming to the regime with a doubly increased time period the scale of the variables x and y is decreased by a times near the extremum points. The relative effect of the perturbation, proceeding along the coupling channel and bypassing the nonlinearity, will be stronger by a times. To compensate the increasing effect of coupling and establish scaling one must decrease the coupling parameter by a times.

Let us now consider the system (4) (Fig. 1b). In multiplying the time scale by two the coefficient $1 - 2\varepsilon$, characterizing the further compression of the phase volume, is raised quadratically. To retain scaling it is necessary to decrease the coupling parameter ε by $b = 2$ times.

In the general case it can be expected that the coupling can be represented in the form of a combination of two components, renormalized during the doubling of the time scale by a and b times, respectively. To justify the suggested scaling law and verify its universality we carry out our study within the renormalized group approach.

2. RENORMALIZED GROUP ANALYSIS

Consider coupled recurrent equations of general form

$$x_{n+1}=f(x_n)+\varphi(x_n, y_n), \quad y_{n+1}=f(y_n)+\varphi(y_n, x_n), \tag{8}$$

where x_n and y_n are the variables characterizing the two identical coupled subsystems, $f(x)$ is a function satisfying the Feigenbaum conditions [1, 2], and $\varphi(x, y)$ is a smooth function of two variables, obeying the condition $\varphi(x, x) \equiv 0$.

We express the values of x_{n+2} and y_{n+2} in terms of x_n and y_n, and carry out the replacement $x \to x/a$, $y \to y/a$. As a result, we obtain

$$x_{n+2}=f_1(x_n)+\varphi_1(x_n, y_n), \quad y_{n+2}=f_1(y_n)+\varphi_1(y_n, x_n),$$

where

$$\begin{gathered} f_1(x)=af(f(x/a)), \\ \varphi_1(x, y)=a[f(f(x/a)+\varphi(x/a, y/a))-f(f(x/a))+\varphi(f(x/a)+\varphi(x/a, y/a), f(y/a)+\varphi(y/a, x/a))]. \end{gathered} \tag{9}$$

Relations (9) define the RG operation of transforming the functions f and φ: $\begin{pmatrix} f_1 \\ \varphi_1 \end{pmatrix}=R\begin{pmatrix} f \\ \varphi \end{pmatrix}$, by means of which is realized the transition to describing the system dynamics with a doubled time interval between successive iterations. By multiple application of the RG transformation we reach the recurrent equation

$$\begin{pmatrix} f_{N+1} \\ \varphi_{N+1} \end{pmatrix} = R\begin{pmatrix} f_N \\ \varphi_N \end{pmatrix}, \tag{10}$$

where f_N and φ_N are the functions determining the change in the system state after 2^N iterations:

$$x_{n+2^N}=f_N(x_n)+\varphi_N(x_n, y_n), \quad y_{n+2^N}=f_N(y_n)+\varphi_N(y_n, x_n). \tag{11}$$

As follows from [1, 2], Eq. (10) has a solution independent of N (a fixed point in function space)

$$\begin{pmatrix} g(x) \\ 0 \end{pmatrix} = R\begin{pmatrix} g(x) \\ 0 \end{pmatrix}, \quad g(x) = ag\left(g\left(\frac{x}{a}\right)\right), \tag{12}$$

where g(x) is the Feigenbaum function. We seek a solution of Eq. (10), adjacent to the fixed point (12), by putting

$$f_N(x)=g(x)+\tilde{f}_N(x),\quad \varphi_N(x,y)=\tilde{\varphi}_N(x,y),\quad |\tilde{f}_N|\ll 1,\quad |\tilde{\varphi}_N|\ll 1.$$

In the linear approximation we obtain from Eq. (10)

$$\begin{pmatrix}\tilde{f}_{N+1}\\ \tilde{\varphi}_{N+1}\end{pmatrix}=\hat{P}\begin{pmatrix}\tilde{f}_N\\ \tilde{\varphi}_N\end{pmatrix}=\begin{pmatrix}\hat{L}&0\\ 0&\hat{M}\end{pmatrix}\begin{pmatrix}\tilde{f}_N\\ \tilde{\varphi}_N\end{pmatrix}, \tag{13}$$

where the linear operators $\hat{L}$ and $\hat{M}$ are determined by the equations

$$\hat{L}f(x)=a[g'(g(x/a))f(x/a)+f(g(x/a))]; \tag{14}$$

$$\hat{M}\varphi(x,y)=a[g'(g(x/a))\varphi(x/a,\ y/a)+\varphi(g(x/a),\ g(y/a))]. \tag{15}$$

To find the general shape of the corrections $\tilde{f}_N$, $\tilde{\varphi}_N$ we turn now to the problem of eigenfunctions and eigenvalues of the operator $\hat{P}$:

$$\nu\begin{pmatrix}\tilde{f}\\ \tilde{\varphi}\end{pmatrix}=\hat{P}\begin{pmatrix}\tilde{f}\\ \tilde{\varphi}\end{pmatrix}. \tag{16}$$

The result of N-fold action of the operator $\hat{P}$ on any vector $\begin{pmatrix}\tilde{f}\\ \tilde{\varphi}\end{pmatrix}$ is represented for large N by a linear combination of those eigenvectors corresponding to values $|\nu| > 1$ which we will call essential. As in [1, 2], we exclude from the treatment the eigenvectors corresponding to infinitesimal replacements of the variables x, y in the fixed point equation (12).

The eigenvectors of the operator $\hat{P}$ can be divided into two classes. The first class consists of vectors of the form $\begin{pmatrix}\tilde{f}\\ 0\end{pmatrix}$, where $\tilde{f}$ are eigenfunctions of the operator (14). This class of eigenvectors refers to the subspace of perturbations of the fixed point (12), not accompanied by inclusion of coupling between subsystems. According to Feigenbaum, there exists a unique eigenvector of the given class $\begin{pmatrix}h(x)\\ 0\end{pmatrix}$ with eigenvalue $\nu = \delta = 4.6692$; the universal function h(x) was calculated in [2].

The second class of eigenvectors form vectors of the shape $\begin{pmatrix}0\\ \tilde{\varphi}(x,y)\end{pmatrix}$, where $\tilde{\varphi}(x, y)$ are eigenfunctions of the operator (15), obeying the condition $\tilde{\varphi}(x, x) = 0$. Perturbations of the fixed point, described by these operators, correspond to the coupling introduced. Numerical solution of the problem of eigenfunctions of the operator (15) (see Appendix 1) showed that there are two substantial eigenfunctions $\Phi_1(x, y)$ and $\Phi_2(x, y)$, possessing the eigenvalues $\nu_1 = a = -2.5029$ and $\nu_2 = b = 2$ (Tables 1 and 2).

Thus, for asymptotically large N the functions f_N and φ_N (see Eq. (11)) have the form

$$f_N(x)=g(x)+\Lambda\delta^N h(x); \tag{17}$$

$$\varphi_N(x,y)=\alpha a^N\Phi_1(x,y)+\beta b^N\Phi_2(x,y), \tag{18}$$

where the shape of the initial perturbation $\tilde{f}_0(x)$, $\tilde{\varphi}_0(x, y)$ determines only the values of the constants Λ, α, β.* Hence follow important conclusions.

*We note that the quantity Λ characterizes the deviation of the Feigenbaum control parameter of the subsystems from the critical point, i.e., $\Lambda = \text{const}(\lambda - \lambda_c)$.

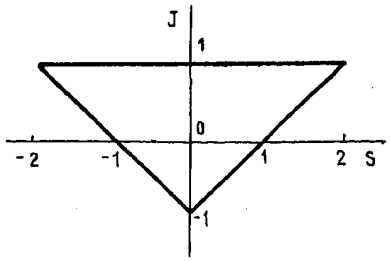

Fig. 2

1. Universality. If the original ("bare") mapping is near the fixed point (12) (i.e., $x_{n+1} = g(x_n)$ + small correction, $y_{n+1} = g(y_n)$ + small correction), then the shape of the mapping describing the dynamic system after a sufficiently large number of iterations is totally determined by the three constants Λ, α, β. Therefore the structure of bifurcation sets in the space of the parameters Λ, α, β is universal and is independent of the specific shape of corrections to the bare mapping.

2. Scaling. At the parameter space point with coordinates $(\Lambda/\delta, \alpha/a, \beta/b)$ the functions $f_{N+1}(x)$ and $\varphi_{N+1}(x, y)$ have exactly the same form as the functions $f_N(x)$ and $\varphi_N(x, y)$ at the point (Λ, α, β). This implies that at the first point the system must demonstrate the same behavior regimes as in the second, but with a time scale multiplied by two. In different words, the structure of the space of parameters possesses the property of scale invariance and transforms into itself, and changes the scales of variation of the three coordinate axes by δ, a, and b times, respectively, which is consistent with the assumptions in the preceding section concerning the scaling hypothesis. Obviously, the first term in the expansion of the coupling function (18) is associated with the inertial, and the second — with the dissipative type of coupling.

3. THE STRUCTURE OF PARAMETER SPACE OF COUPLED SYSTEMS

To study the universal structure of the parameter space of coupled systems one can use the model considered above (6) or use a different notation (7). Indeed, from the qualitativw considerations of Sec. 1 follows the existence in this model of both inertial and dissipative coupling. The presence of the two coupling parameters ε and μ makes it possible to assign an arbitrary relation between both coupling types. It is shown in Appendix 2 that a formulation of the equations admitting an independent control level of both pure coupling types is obtained by putting in Eq. (7) $B = e^{-\beta F(\alpha, \lambda)}$:

$$\xi_{n+1} = \lambda - \xi_n^2 - \eta_n^2, \quad \eta_{n+1} = -2e^{-\beta F(\alpha, \lambda)}(\xi_n + \alpha)\eta_n, \tag{19}$$

where α and β are the coupling coefficients of the inertial and dissipative types, while the function $F(\alpha, \lambda)$ is approximately expressed by the equation

$$F(\alpha, \lambda) = (1 - 0.6025\alpha + 0{,}1019\alpha^2 - 0{,}0278\alpha\lambda)^{0{,}2779}. \tag{20}$$

The starting moment of studying the structure of the system parameter space is the analysis of periodic regimes (cycles).

3. Cycles and Their Stability. We assume that for several values of the system parameters there exists an N-cycle, i.e., a solution for which $\xi_{n+N} = \xi_n$, $\eta_{n+N} = \eta_n$. For stability analysis one usually considers the evolution of increments $\tilde{\xi}_n$, $\tilde{\eta}_n$ to the variables ξ_n, η_n following a period of the cycle. As follows from Eq. (19)

$$\begin{pmatrix} \tilde{\xi}_N \\ \tilde{\eta}_N \end{pmatrix} = J \begin{pmatrix} \tilde{\xi}_0 \\ \tilde{\eta}_0 \end{pmatrix}, \tag{21}$$

where $\hat{J}=\hat{J}_{N-1}\hat{J}_{N-2}\ldots\hat{J}_0$ is the matrix of a monodrome cycle, and $\hat{J}_n$ is the Jacobi matrix of mapping (19) at the n-th point of the cycle,

$$\hat{J}_n=\begin{pmatrix}-2\xi_n & -2\eta_n\\ -2B\eta_n & -2B(\xi_n+\alpha)\end{pmatrix}. \tag{22}$$

The eigenvalues of the matrix $\hat{J}$ (multipliers) are determined from the equation

$$\mu^2-\mu S+J=0, \tag{23}$$

where S is the trace and J is the determinant of the matrix $\hat{J}$. In the (S, J) plane the stability region of the cycle ($|\mu| < 1$) is mapped by a triangle (Fig. 2) with sides

$$1)\ J+S+1=0,\quad 2)\ J-S+1=0,\quad 3)\ J=1. \tag{24}$$

Passing through each of the three sides of the triangle corresponds to 1) period doubling bifurcation of the cycle, 2) tangential bifurcation, and 3) bifurcation of quasiperiodic attractor creation (Andronov–Hopf bifurcation). Tracking the cycle evolution during variation of the problem parameters, and calculating the trace and determinant of the monodrome matrix, one can find the bifurcation surfaces of the three enumerated types in the parameter space (λ, α, β).

We note that the original equations admit solution in the form of cophase subsystem motions, i.e.,

$$x_n\equiv y_n \quad \text{or} \quad \eta_n\equiv 0. \tag{25}$$

In this case the problem reduces to Eq. (2). Therefore, according to [1, 2], for $\lambda < \lambda_c = 1.40116$ there exist cophase cycles of period 2^m, while cophase chaotic regimes occur for $\lambda > \lambda_c$. For cophase cycles the matrices $\hat{J}_n$ and consequently $\hat{J}$ are diagonal; therefore the eigenvalues are simply the diagonal elements of the matrix $\hat{J}$:

$$\mu_1=\prod_{n=1}^{N}(-2\xi_n),\quad \mu_2=\prod_{n=1}^{N}(-2B(\xi_n+\alpha)),$$

where N is the cycle period. The stability condition is

$$\left|\prod_{n=1}^{N}(-2\xi_n)\right|<1,\quad \left|\prod_{n=1}^{N}(-2B(\xi_n+\alpha))\right|<1 \tag{26}$$

while for cycles of period 1 and 2 it is expressed explicitly, since

$$\text{for } N=1\text{: } \mu_1=1-\sqrt{1+4\lambda},\quad \mu_2=B(1+\alpha-\sqrt{1+4\lambda}; \tag{27}$$

$$\text{for } N=2\text{: } \mu_1=4-4\lambda,\quad \mu_2=4B^2(1-\lambda+\alpha+\alpha^2). \tag{28}$$

3.2. A System with Purely Dissipative Coupling. We put in Eq. (19) $\alpha = 0$. Taking into account that $F(0, \alpha) = 1$, we have

$$\xi_{n+1}=\lambda-\xi_n^2-\eta_n^2,\quad \eta_{n+1}=-2e^{-\beta}\xi_n\eta_n. \tag{29}$$

We consider only the case $\beta > 0$ (the dissipation condition).

For $\lambda < \lambda_c$ the behavior of system (29) is very simple: it demonstrates stable cophase cycles, whose period doubles for the same λ_m values as for the isolated Feigenbaum system (2). Indeed, it is seen from Eq. (26) that the first multiplier of the cophase 2^m-cycle coincides with the multiplier system (2), while the second equals $\mu_2=\mu_1 e^{-2^m\beta}$. In the existence region of the given cycle, as in that of the attractor of system (2), $|\mu|_1 < 1$, therefore also $|\mu_2| < 1$. Consequently, the cycle of system (29) is stable in the same interval of the parameter λ as is the cycle of system (2). Therefore, on the parameter plane (β, λ) the regions of cycles of a different period, realized for $\lambda < \lambda_c$, are bounded by the horizontal lines $\lambda = \lambda_m$ (Fig. 3).

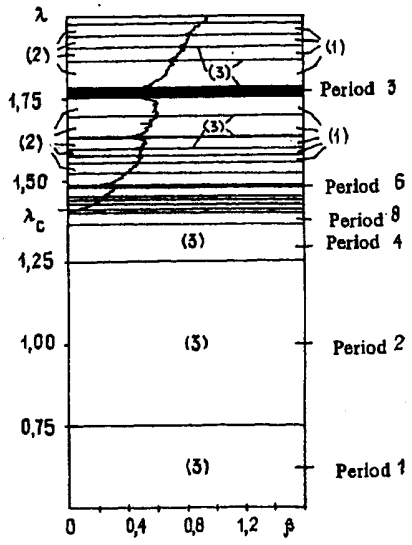

Fig. 3

For $\lambda > \lambda_c$ the cophase regime can lose stability to antisymmetric perturbations if the Lyapunov characteristic index, calculated for the strange attractor of system (2),

$$\gamma = \lim_{N\to\infty} \frac{1}{N} \sum_{n=1}^{N} \ln |2x_n|,$$

becomes larger than β [14]. For $\lambda > \lambda_c$ there exist regions of three types in the parameter plane: 1) zones of cophase chaotic motion, determined by the condition $0 < \gamma(\lambda) < \beta$, 2) instability zones of a cophase chaotic regime, in which $\gamma(\lambda) > \beta$, and noncophase subsystem stochastic oscillations are realized, and 3) stability zones of periodic motions, coinciding with the "stability windows" in the post-critical region of system (2) [1, 2]. The coefficients of all these regions can be found by using the well-known dependence $\gamma(\lambda)$ for the system (2) [15]. We note that the pattern of regions in Fig. 3 transforms into itself when the scale changes by δ times along the λ axis, and by $b = 2$ times along the β axis with respect to the point $(0, \lambda_c)$. Thus is expressed the scaling law for a system with dissipative coupling.

3.3. A System with Pure Inertial Coupling. We put now $\beta = 0$ and consider the behavior of system (19) as a function of the parameters α (the coupling coefficient) and λ (the Feigenbaum control parameter). Since hysteresis effects are possible in a system with inertial coupling, it is useful to represent the surface (α, λ) as a sequence of glued sheets (Fig. 4a). One of them, denoted as the S-sheet, corresponds to cophase motions of subsystems, while the remaining N-sheets — to noncophase motions. If the intersection of some bifurcation line leads to a soft transition from one sheet to another, then both sheets are assumed glued along this line (see Fig. 4a, transition 1). The nonglued sheet edges reflect the existence of rigid bifurcation — a jump from one sheet to another, accompanied by hysteresis (transition 2 in Fig. 4a). Figure 4a provides a crude preliminary concept on the structure of parameter space. We turn now to discuss it in detail.

The S-Sheet. Consider cophase periodic motion in the region $\lambda < \lambda_c$. From Eq. (26) one can numerically find the boundaries of the stability region of 2^m-cycles. To these belong: 1) the horizontal lines $\lambda = \lambda_m$, determined by the condition $\mu_1(\lambda) = -1$ and corresponding to the bifurcation conditions of the period of cophase cycles, and 2) the curves assigned by the relations $\mu_2(\lambda, \alpha) = \pm 1$, corresponding to stability loss of the cophase regime with respect to an antisymmetric perturbation and transition to any N-sheet. Both families of the bifurcation lines on the S-sheet are illustrated in Fig. 4b. In the lighted areas are realized stable cophase cycles with a period indicated in the figure, and the instability regions of cophase regimes are shaded. The line on which the S-sheet is glued to N-sheets consists of the lowest arched boundaries of the shaded areas, on which $\mu_2 = -1$.

We note the following scaling property which is clearly fixed in numerical computations: the whole region pattern in Fig. 4b is reproduced inside the rectangle, denoted by dots, with a scale decreased δ times along the ordinate axis and a times along the abscissa axis. Since

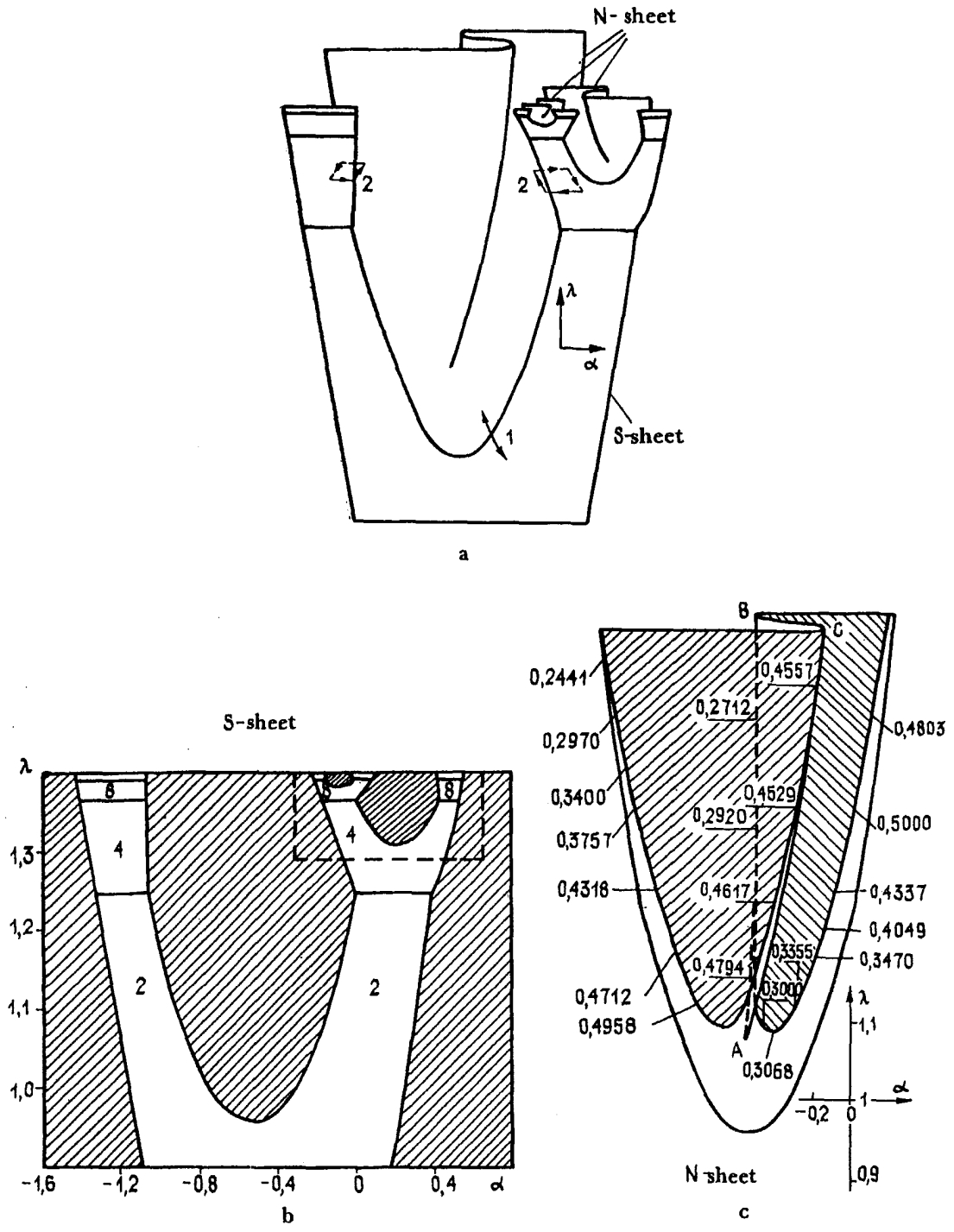

Fig. 4

the constant a is negative, the location of regions in large and small rectangles is opposed in orientation to the abscissa axis.

N-Sheets. We study now the regions of noncophase motions, realized on N-sheets. Due to the existence of a scaling law it is sufficient to study the structure of a single N-sheet, one on which is realized a transition during a soft stability loss of a cophase 2-cycle.

The N-sheet under consideration is glued to an S-sheet along the line determined by Eqs. (26) and (28): $4B^2(1 - \lambda + \alpha + \alpha^2) = -1$, $\lambda < 1.25$. During transition through it from below upwards there is a stability bifurcation creation of a 4-cycle, corresponding to motion of both subsystems, phase shifted with respect to each other by half a period:

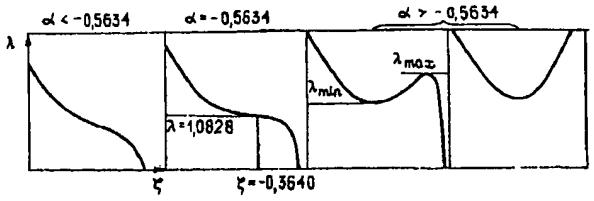

Fig. 5

$$x_{n+2}=y_n,\quad y_{n+2}=x_n \quad \text{or} \quad \xi_{n+2}=\xi_n,\quad \eta_{n+2}=-\eta_n, \tag{30}$$

This cycle can be studied analytically: introducing the quantity $\zeta = \xi_1 + \xi_2 + 2\alpha$, the cycle elements and the parameter λ are expressed in terms of ζ:

$$\xi_{1,2}=(1/2)(\zeta\pm\sqrt{\zeta^2+B^{-2}})-\alpha,\quad \eta_{1,2}=\sqrt{C(1+\alpha A+A\xi_{1,2})}; \tag{31}$$

$$\lambda=C+\zeta+1/4B^2+\alpha^2-\alpha, \tag{32}$$

where $A = -(\zeta + 1/2\zeta B^2)^{-1}$, $B = F(\alpha, \lambda)$, $C = (1 + 2\alpha - \zeta)/A$.* The multipliers are calculated by the usual equations (21)-(23). Different bifurcations can occur with the cycle (30), which we now consider.

1) Assembly Point and Folding Line. It is shown in Fig. 5 how the curve $\lambda = \lambda(\zeta)$ (32) evolves with variation of the parameter α. For $\alpha < -0.5634$ there exists one, while for $\alpha > -0.5634$ and $\lambda_{min} < \lambda < \lambda_{max}$ — three ζ values for a single λ. Consequently, in the first case there exists one, and in the second — three different 4-cycles of type (30). Among these cycles one is always unstable (it corresponds to the mean ζ value), while the two others are stable in a definite parameter region and can be observed as attractors. Thus, at the point $\alpha = -0.5634$, $\lambda = 1.0829$ there exists assembly bifurcation [16]. At this point of the surface (α, λ) there are two folding lines [16] corresponding to the extrema of the curve $\lambda(\zeta)$ in Fig. 5. This line can be found by supplementing Eq. (32) by the condition $\partial\lambda/\partial\zeta = 0$. In Fig. 4c, illustrating the structure of the N-sheet, the point A is an assembly point, while the lines BA and CA are folding lines. In by-passing the point A clockwise the attractor (a 4-cycle) evolves continuously till the intersection with the line CA, following which there is a jumpwise regime replacement. This is again a 4-cycle obeying condition (30), but differing from the old level of the antisymmetric mode η. In by-passing the point A counterclockwise, the jump occurs during intersection of the line BA. As can be verified, on the folding lines one of the multipliers of the 4-cycles becomes +1. At the assembly point the multipliers are: $\mu_1 = 1$, $\mu_2 = 0.1472$.

2) Andronov–Hopf Bifurcation Line and Transition to a Quasiperiodic Attractor. In Fig. 4c one sees two shaded regions, lying in two portions of the N-sheet surface, matched at the assembly point. In these regions the determinant of the monodrome matrix of the 4-cycle (30) exceeds unity, i.e., the cycle is unstable (Sec. 3.1). At the boundaries of the shaded areas the determinant equals unity, which corresponds to Andronov–Hopf bifurcation (a transition of a pair of complex-conjugate multipliers through a unit cycle) with creation of a quasiperiodic attractor. Along with the bifurcation lines are shown the values of the rotation cycle — period ratios of the original to the newly generated motions.

The shaded areas have a fine structure in the form of synchronization laws, resting on points of the bifurcation lines with rational rotational numbers, and a residual set corresponding to quasiperiodic motion [17]. This structure was not investigated by us in any detail, and is not shown in the figure.

3) Edge of the N-Sheet: Lines of Tangential Bifurcation. On both boundaries of the N-sheet shown in Fig. 4c one of the multipliers of the 4-cycle (30) becomes +1. During intersection of any of these boundaries at the point $(\alpha, \lambda < \lambda_c)$ there is a jumplike transition to the cophase regime, illustrated by a point with the very same coordinates, but on

*Due to the fact that $B = F(\alpha, \lambda)$, relationship (32) is an equation in λ. However, the dependence $B(\lambda)$ is weak; therefore, for sufficiently accurate determination of λ it is sufficient to iterate Eq. (32) once or twice.

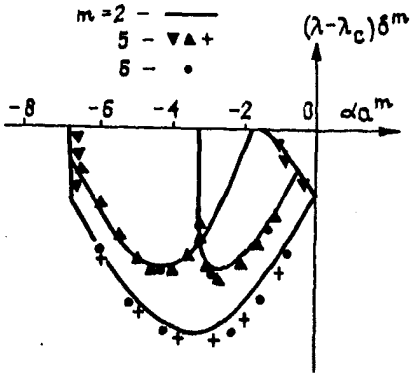

Fig. 6

the S-sheet. In this case there is hysteresis: the inverse jump on the N-sheet occurs only during intersection of the lateral boundary of the stability region of the cophase regime, which does not coincide with the edge of the N-sheet.

Due to the scaling law, effects similar to those descrbed in paragraphs 1)-3) must also occur in N-sheets, glued to the lower arched boundaries of the small regions shaded in Fig. 4b. Figure 6 shows results of quantitative verification of the scaling shape of bifurcation lines on different N-sheets. These lines must coincide in the coordinates $(\alpha a^m, (\lambda - \lambda_c)\delta^m)$, where 2^m is the period of the cycle created during the soft transition on the sheet under consideration. As seen from Fig. 6, the results for m = 2, 5, and 6 are in good agreement. The same conclusions on the behavior of the system on the N-sheet, obtained for m = 2, also extend to the remaining N-sheets; the difference consists only of changing the time scale of motion.

The constructed "geographic map" of the surface of the parameters (α, λ) provides a fairly complete concept on the different possible transition paths to chaos in a system with inertial coupling. In the original state let there be selected some point on the S-sheet for $\lambda < \lambda_c$. Moving, then, along the surface (α, λ) in the general direction of increasing λ, one can observe, for example, these scenarios of chaos generation:

1) An infinite sequence of period doubling of cophase motions (Fig. 7, path 1).

2) An arbitrary finite number of period doublings of cophase cycles, then period doubling with the appearance of a noncophase cycle and two variants of further evolution:

a) Andronov–Hopf bifurcation with the creation of quasiperiodic motion, its destruction and transition to chaos (Fig. 7, path 2).

b) Jumpwise transition to an S-sheet and subsequent repetition of the effects described in paragraphs 1) or 2) (Fig. 7, paths 3 and 4).

3.4. A System with Combined Coupling. In the case of combined coupling the number of substantial coupling parameters increases to three, so that a smooth mapping of the structure of the parameter space becomes hindered. Therefore we restrict ourselves to a qualitative description only.

We pretend that in a system with a purely inertial coupling type one introduces an additional, dissipative coupling, and proceeds to the pattern evolution behind the surface (α, λ). Calculations show that for small dissipative coupling the structure of this surface is retained in the form of glued N- and S-sheets, as well as the general location of regions on these sheets. Increases in dissipative coupling are initially small, and therefore large instability zones of cophase regimes occur from above and disappear in the region $\lambda > \lambda_c$. To have each successive branch vanish, the dissipative coupling parameter must be multiplied by a factor of two. Finally, an increase in dissipative coupling leads to the fact that the subcritical system behavior and the character of transition to chaos become the same as described in Sec. 3.2.

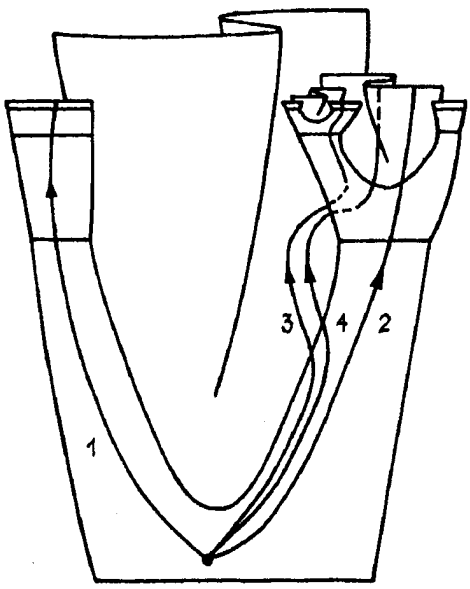

Fig. 7

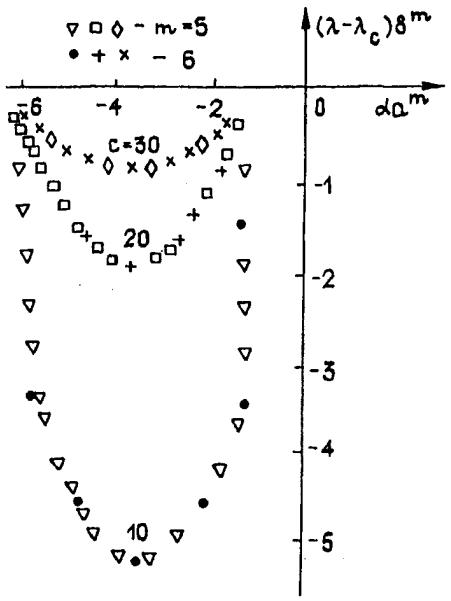

Fig. 8

To verify the scaling relations consider the cross section of the parameter space (λ, α, β) with the surface

$$\beta = c|\lambda - \lambda_c|^{\log \delta}, \tag{33}$$

where c is an arbitrary constant. With a scale varying along the λ axis by δ times and along the α axis by a times the quantity β changes by a factor of two, and therefore the configuration of regions on the given surface must transform into itself. Figure 8 shows the lines of stability loss of cophase 2^m-cycles on the surface (33) for several c values in the coordinates $(\alpha a^m, (\lambda - \lambda_c)\delta^m)$. Good agreement of the data is observed for different m.

Based on the study performed above, the following may be concluded:

1) The existence of Feigenbaum properties for the component elements leads to the fact that the universality and scaling laws also occur in dynamics of coupled systems.

2) Universality is expressed by the fact that any weak coupling, introduced by means of an arbitrary smooth function of state elements, is totally characterized by the two constants α and β, the coefficients of inertial and dissipative coupling types. Therefore, a full description of coupled systems near the transition point to chaos is achieved by assigning the three parameters λ, α, β, where λ is the Feigenbaum parameter of the subsystems

3) The structure of bifurcation sets in the parameter space λ, α, β obeys the scaling law, and transforms into itself with the following scale changes along the three coordinate axes, respectively, $\delta = 4.6692$, $a = -2.5029$ and $b = 2$ times. This universal, three-dimensional structure contains surfaces of bifurcation doubling, tangential bifurcation, and bifurcation of quasiperiodic motion creation.

Due to the universality of the laws considered, the results obtained can also refer to a wide class of coupled systems of differing orders, described by both mapping and differential equations.

APPENDIX 1

For numerical solution of the problem of eigenfunctions of the operator $\hat{M}$ (see Eq. (15)) we used an iteration method consisting of the following. As is easily verified, the result of N-fold action of the operator $\hat{M}$ on the function $\varphi(x, y)$ can be calculated by the equations

$$\hat{M}^N\varphi = a^N\xi_{2^N}, \quad \xi_{n+1} = g'(x_n)\xi_n + \varphi(x_n, y_n), \quad x_{n+1} = g(x_n), \quad y_{n+1} = g(y_n),$$
$$x_0 = x/a^N, \quad y_0 = y/a^N, \quad \xi_0 = 0,$$

TABLE 1. The Eigenfunction $\Phi_1(x, y)$

y	x								
	—1,00	—0,75	—0,50	—0,25	0	0,25	0,50	0,75	1,00
—1,00	0,0000	—0,1713	—0,3447	—0,5133	—0,6723	—0,8158	—0,9322	—1,0024	—1,0000
—0,75	0,1611	0	—0,1676	—0,3334	—0,4916	—0,6358	—0,7550	—0,8311	—0,8389
—0,50	0,3110	0,1611	0	—0,1638	—0,3199	—0,4650	—0,5875	—0,6702	—0,6890
—0,25	0,4506	0,3128	0,1589	0	—0,1562	—0,3025	—0,4285	—0,5183	—0,5494
0	0,5804	0,4556	0,3097	0,1549	0	—0,1475	—0,2777	—0,3755	—0,4196
0,25	0,7006	0,5898	0,4526	0,3024	0,1489	0	—0,1348	—0,2413	—0,2994
0,50	0,8110	0,7151	0,5875	0,4424	0,2904	0,1399	0	—0,1160	—0,1890
0,75	0,9111	0,8311	0,7136	0,5740	0,4238	0,2716	0,1261	0	—0,0889
1,00	1,0000	0,9368	0,8302	0,6966	0,5482	0,3941	0,2427	0,1057	0

TABLE 2. The Eigenfunction $\Phi_2(x, y)$

y	x				
	0	0,25	0,50	0,75	1,00
0	0	−0,0658	−0,2584	−0,5598	−0,9316
0,25	0,0659	0	−0,1931	−0,4958	−0,8697
0,50	0,2612	0,1948	0	−0,3064	−0,6871
0,75	0,5774	0,5102	0,3126	0	−0,3921
1,00	1,0000	0,9316	0,7280	0,4082	0

Note. The function $\Phi_2(x, y)$ is even in both arguments.

where $n = 0, 1, \ldots, 2^N - 1$. Assigning an arbitrary bare function $\varphi(x, y)$, and calculating $\hat{M}^N\varphi$ for different x, y, and N, it can be expected that $\hat{M}^N\varphi \xrightarrow[N\to\infty]{} \nu^N\Phi(x, y)$. Here $\Phi(x, y)$ is the eigenfunction corresponding to the eigenvalue ν, maximum in absolute value among the components of $\varphi(x, y)$.

Such calculations were carried out for N = 2-6; the functions g(x) and g'(x) were calculated by means of polynomial approximations [2]. As bare functions we used the functions $\varphi(x, y) = (x - y)\psi(x, y)$, where $\psi(x, y) = 1, x, y, x^2, xy, y^2, x^3, x^2y, xy^2, y^3$. (As is well known, linear combinations of power monoterms by a Taylor series can be represented by an arbitrary smooth function.) When assigning $\psi(x, y) = 1$ the result of the iteration procedure is the eigenfunction $\Phi_1(x, y)$ (Table 1) and the eigenvalue $\nu_1 = a = -2.5029$. For the remaining $\psi = x^m y^n$ the iterations led to the eigenfunction $\Phi^2(x, y)$ (Table 2) with eigenvalue $\nu_2 = b = 2$. It can be shown that the equalities $\nu_1 = a$ and $\nu_2 = 2$ are accurate.

From the equation $\nu\Phi = \hat{M}\Phi$ with account of (15) we have for the function $F(x) = \left[\frac{\partial\Phi(x, y)}{\partial y}\right]_{y=x}$

$$\nu F(x) = g'(g(x/a))F(x/a) + g'(x/a)F(g(x/a))$$

— an equation sufficient for the determination of eigenvalues. This equation was analyzed in [13], where it was shown rigorously that the old eigenvalues are $\nu_1 = a$ and $\nu_2 = 2$.

The remaining term, obtained in approximating $\hat{M}^N\varphi$ by a linear combination of the functions $\Phi_1(x, y)$ and $\Phi_2(x, y)$, consists of two parts, one damped for $N \to \infty$, and the other undamped. The latter is given by the eigenfunction $\Phi_3(x, y) = g'(x)(y - x) - g(y) + g(x)$ with eigenvalue $\nu_3 = 1$, and is removed by the variable replacement $x \to x + (y - x)\text{const}$, $y \to y + (x - y)\text{const}$.

APPENDIX 2

It seems that purely dissipative coupling is realized in system (4), while system (5) displays a combination of both coupling types, understood in the sense of Sec. 2. A system with a purely inertial coupling type can be constructed, assigning in (7) a parameter dependence $B = F(\alpha, \lambda)$, so that a scaling law characteristic of inertial coupling be best satisfied. We use this idea for approximate calculation of the function $F(\alpha, \lambda)$. Consider a cophase cycle of period 2:

$$\xi_1 = \lambda - \xi_0^2, \quad \xi_2 = \lambda - \xi_1^2, \quad \eta_0 = \eta_1 = 0, \tag{A.2.1}$$

whose multipliers are determined by Eqs. (28). We require that for some value of the parameter λ_1 and a coupling decreased by a times, i.e., for $\alpha_1 = \alpha/a$, $B_1 = B^1/a$, there exist a cophase 4-cycle $\xi_0, \xi_1, \xi_2, \xi_3, \eta_n \equiv 0$, obeying the scaling relations $\xi_0 = \xi_0/a$, $\xi_2 = \xi_1/a$, and possessing numerically the same multipliers as does the 2-cycle (A.2.1). For the multipliers of the 4-cycle we have

$$\mu_1 = 16(\xi_0/a)(\xi_1/a)(\lambda_1 - \xi_0^2/a^2)(\lambda_1 - \xi_1^2/a^2); \tag{A.2.2}$$

$$\mu_2 = 16(B^{4/a}/a^2)(\xi_0 + \alpha)(\xi_1 + \alpha)(\lambda_1 - \xi_0^2/a^2 + \alpha/a) \quad (\lambda_2 - \xi_1^2/a^2 + \alpha/a). \tag{A.2.3}$$

Equating the μ_1 values of (A.2.2) and (28), we obtain a relation between λ and λ_1, which reduces with high accuracy to the equation

$$\lambda_1=\lambda_c+(\lambda-\lambda_c)\delta^{-1}. \qquad (A.2.4)$$

The equality requirement of the multipliers μ_2 leads, with account of (A.2.1)-(A.2.4) and Eq. (28), to the expression

$$B=[1+8(\lambda_1-\lambda/a^2)\alpha a^{-3}+4\alpha a^{-4}(\alpha+1/a)]^{a/(2a-4)}.$$

Hence, using (A.2.4), and substituting the numerical values of α, δ and λ_c, we reach Eq. (20). Putting in Eq. (7) $B = e^{-\beta F(\alpha, \lambda)}$, we obtain a system in which the inertial and dissipative coupling are regulated by the independent parameters α and β.

LITERATURE CITED

1. M. Feigenbaum, Usp. Fiz. Nauk, 141, No. 2, 343 (1983).
2. M. J. Feigenbaum, J. Stat. Phys., 19, No. 1, 25 (1978); 21, No. 6, 669 (1979).
3. J. P. Eckmann, Rev. Mod. Phys., 53, No. 4, 643 (1981).
4. J. Testa, J. Perez, and C. Jeffries, Phys. Rev. Lett., 48, No. 11, 714 (1982).
5. A. Libchaber, S. Fauve, and C. Laroche, Physica, 7D, 73 (1983).
6. T. Kai, Phys. Lett., 86A, No. 5, 263 (1981).
7. R. May, Nature, 261, 459 (1976).
8. S. P. Kuznetsov, Pis'ma Zh. Eksp. Teor. Fiz., 39, No. 3, 113 (1984).
9. K. Kaneko, Prog. Theor. Phys., 69, No. 5, 1427 (1983).
10. Jian-Min Yuan, Mingwhei Tung, Da Hsuan Feng, and Lorenzo M. Norducci, Phys. Rev., A28, No. 3, 1662 (1983).
11. R. King, J. D. Barchas, and B. Huberman, in: Synergetics of the Brain, Springer-Verlag (1983), p. 352.
12. S. P. Kuznetsov, Pis'ma Zh. Tekh. Fiz., 9, No. 2, 94 (1983).
13. S. P. Kuznetsov, Izv. Vyssh. Uchebn. Zaved., Fiz., 27, No. 6, 87 (1984).
14. A. S. Pikovskii, Preprint No. 79 IPF AN SSSR, Gorki (1983).
15. T. Geisel, J. Nierwetberg, and J. Keller, Phys. Lett., 86A, No. 2, 75 (1981).
16. T. Poston and I. Stewart, Catastrophe Theory and Its Applications, Pitman, San Francisco (1978).
17. V. I. Arnol'd, The Theory of Ordinary Differential Equations [in Russian], Nauka, Moscow (1978).